

# Control of river stage on the reactive chemistry of the hyporheic zone

P. Byrne,<sup>1,\*†</sup> A. Binley,<sup>1</sup> A. L. Heathwaite,<sup>1</sup> S. Ullah,<sup>1,‡</sup> C. M. Heppell,<sup>2</sup> K. Lansdown,<sup>2,3</sup> H. Zhang,<sup>1</sup> M. Trimmer<sup>3</sup> and P. Keenan<sup>1</sup>

<sup>1</sup> Lancaster Environment Centre, Lancaster University, Lancaster LA1 4YQ, UK

<sup>2</sup> School of Geography, Queen Mary University of London, London E1 4NS, UK

<sup>3</sup> School of Biological and Chemical Sciences, Queen Mary University of London, London E1 4NS, UK

## Abstract:

We examined the influence of river stage on subsurface hydrology and pore water chemistry within the hyporheic zone of a groundwater-fed river during the summer baseflow period of 2011. We found river stage and geomorphic environment to control chemical patterns in the hyporheic zone. At a high river stage, the flux of upwelling water in the shallow sediments (>20 cm) decreased at sample sites in the upper section of our study reach and increased substantially at sites in the lower section. This differential response is attributed to the contrasting geomorphology of these subreaches that affects the rate of the rise and fall of a river stage relative to the subsurface head. At sites where streamward vertical flux decreased, concentration profiles of a conservative environmental tracer suggest surface water infiltration into the riverbed below depths recorded at a low river stage. An increase in vertical flux at sites in the lower subreach is attributed to the movement of lateral subsurface waters originating from the adjacent floodplain. This lateral-moving water preserved or decreased the vertical extent of the hyporheic mixing zone observed at a low river stage. Downwelling surface water appeared to be responsible for elevated dissolved organic carbon (DOC) and manganese (Mn) concentrations in shallow sediments (0–20 cm); however, lateral subsurface flows were probably important for elevated concentrations of these solutes at deeper levels. Results suggest that DOC delivered to hyporheic sediments during a high river stage from surface water and lateral subsurface sources could enhance heterotrophic microbial activities. Copyright © 2013 John Wiley & Sons, Ltd.

**KEY WORDS** hyporheic zone; river stage; pore water; nutrients; biogeochemistry; dissolved organic carbon

Received 10 March 2013; Accepted 15 July 2013

## INTRODUCTION

As the interface between surface and groundwater, the hyporheic zone of riverbed sediments is recognized as a critically important ecotone (Boulton, 2007) where water, organic matter and energy transfer takes place at a range of spatial and temporal scales (Wrobleckiy *et al.*, 1998). The dynamic flux of oxygen, carbon and nutrients, increased microbial activity, and elevated water temperatures can create steep hydrological and chemical gradients in the hyporheic zone leading to active biogeochemical zones in the streambed where nutrient attenuation and/or release can occur (Krause *et al.*, 2009; Mulholland *et al.*, 2009).

Stream nutrient processing and the location of active biogeochemical zones in the hyporheic zone may be dependent on streambed hydrological connectivity and patterns of hyporheic exchange flow (HEF; vertical, lateral and longitudinal) that control the mixing, transport and patterns of redox-sensitive species (Käser *et al.*, 2009). Hyporheic exchange flows, in turn, are controlled by differences in hydraulic head gradients and hydraulic conductivity (Kasahara and Wondzell, 2003).

As climate change models predict warmer and drier summers, water resources and nutrient yields could be significantly affected (Rance *et al.*, 2012). This has put an emphasis on understanding nutrient transformation processes in the hyporheic zone and the interrelationships with groundwater flux. In response, a plethora of studies (both field and modelling) have increased our understanding of surface–subsurface water exchange processes (e.g. Käser *et al.*, 2009; Boano *et al.*, 2011; Munz *et al.*, 2011; Briggs *et al.*, 2012) and biogeochemical aspects (e.g. Lautz and Fanelli, 2008; Krause *et al.*, 2009; Zarnetske *et al.*, 2011a).

\*Correspondence to: P. Byrne, Lancaster Environment Centre, Lancaster University, Lancaster LA1 4YQ, UK.

E-mail: p.a.byrne@lmu.ac.uk

†Current Address: School of Psychology and Natural Sciences, Liverpool John Moores University, Liverpool L3 3AF, UK

‡Current Address: School of Physical and Geographical Sciences, Keele University, Keele ST5 5BG, UK

of the hyporheic zone. Climate change models also predict intensified storm activity during summer periods leading to increased frequency and magnitude of high flow events (Rance *et al.*, 2012). Several field and modelling studies (e.g. Cardenas and Wilson, 2007; Gu *et al.*, 2008a; Westhoff *et al.*, 2011) have observed expansion of the hyporheic zone during high river stage periods driven by downwelling surface water. Evidence suggests that this downwelling surface water may lead to longer water residence times in the hyporheic zone and enhanced nutrient cycling (Gu *et al.*, 2008b); however, the biogeochemical implications of river stage variability remain relatively unknown.

The work presented here is part of a larger project investigating groundwater surface water connectivity for nitrogen transformations in the hyporheic zone of a gaining reach in the River Eden, Cumbria, UK. We have instrumented a 200-m reach with a dense network of channel and riparian piezometers allowing us to establish spatial and temporal patterns of groundwater-surface water exchange linked to redox-sensitive chemical patterns that determine nitrate transport and transformation in the hyporheic zone. Previous work at the site has allowed us to conceptualize hydrological flow paths at the groundwater-surface water interface under baseflow conditions (Binley *et al.*, submitted for review; Lansdown *et al.*, submitted for review). This work has revealed a localized connectivity to regional groundwater with only limited downwelling in some parts of the river, potentially limiting any hyporheic zone-driven attenuation of nitrate. We have used this conceptual understanding of hydrological connectivity under baseflow conditions to address spatial patterns in redox-sensitive chemistry and nitrogen dynamics in the hyporheic zone. We have found that patterns in redox-sensitive chemistries reflect the spatial variability of different sources of water flux in the streambed, with oxic conditions associated with upwelling preferential groundwater and reduced conditions associated with areas of the streambed dominated by fluxes of lateral and longitudinal subsurface water (Heppell *et al.*, in prep). Patterns of nitrate removal from upwelling groundwater are explained by the mixing of downwelling surface water and upwelling pore water; the supply of labile DOC from downwelling surface water enhances microbial respiration and fuels reduction of nitrate (Lansdown *et al.*, submitted for review). These investigations have allowed us to develop a conceptual model linking hydrological connectivity and biogeochemical process under baseflow or low stage conditions. However, under high river stage, we may see deeper mixing and thus 'priming' of the subsurface through a temporary expansion of the hyporheic zone that would ultimately affect the extent and rate of chemical transformations through changes in the supply of redox-sensitive solutes at depth (Zarnetske *et al.*, 2011b; Stelzer and Bartsch, 2012). A previous study

in part of our study reach (Käser *et al.*, 2009) provided some evidence that increases in river stage during high river stage events will cause predominant upwelling hydraulic flow paths (vertical) to weaken or even to reverse at some locations. In this paper, we hypothesize that disturbances to hydraulic exchange of surface and subsurface waters as a result of increased river stage will affect the depth of surface-subsurface water mixing and hence spatial patterns of reactive redox-sensitive solutes in the hyporheic zone. Our specific objectives were the following: (1) investigate subsurface water flux and chemical patterns in the streambed at the reach scale; (2) examine the change in these patterns during increased river stage; and (3) characterize hydrological and chemical zones in the streambed by using multivariate statistical methods.

## METHODS

### Study site

This investigation was conducted on the River Leith, a tributary of the River Eden, Cumbria, UK (Figure 1). The River Leith catchment (54 km<sup>2</sup>) lies on Permo-Triassic sandstone overlain by glaciofluvial sediments, typically to a depth of up to 2 m. The investigated reach is 200-m long (Figure 1) and meanders in a narrow floodplain (<100 m) comprising agricultural and pastoral landscape. Stream channel morphology is characterized by riffle-pool sequences of predominantly gravel and cobble substrate overlying unconsolidated sands and silts. The study reach lies in a 5 km section of the River Leith that is net-gaining groundwater (Krause *et al.*, 2009). River stage and discharge is recorded by the Environment Agency of England and Wales at Cliburn weir (N54:37:03; W2:38:23), approximately 50 m downstream of the study reach. From 2004 to 2011, the mean daily discharge in summer (1 June to 30 September) was 0.68 m<sup>3</sup>/s.

### Field and laboratory methods

The research undertaken here covers the baseflow period in 2011 (1 June to 30 September). During this period, mean daily river discharge ranged between 0.07 and 4.98 m<sup>3</sup>/s with a mean of 0.44 m<sup>3</sup>/s. Precipitation data were provided by an Environment Agency tipping bucket rain gauge at Kirkby Thore, near Penrith (64:39:10E; 26:71:00N), approximately 5 km east of the study reach. Mean daily precipitation during the study period was 4.9 mm. The maximum daily precipitation was 22.6 mm on 6th August. Hydrological and chemical data were collected on two low stage days (mean 0.43 m (0.08 m<sup>3</sup>/s) and 0.45 m (0.10 m<sup>3</sup>/s)) in July 2011 and on two high stage days (mean 0.64 m (0.94 m<sup>3</sup>/s) and 0.69 m (1.39 m<sup>3</sup>/s)) in September 2011 (Figure 2). The lowest and highest stage

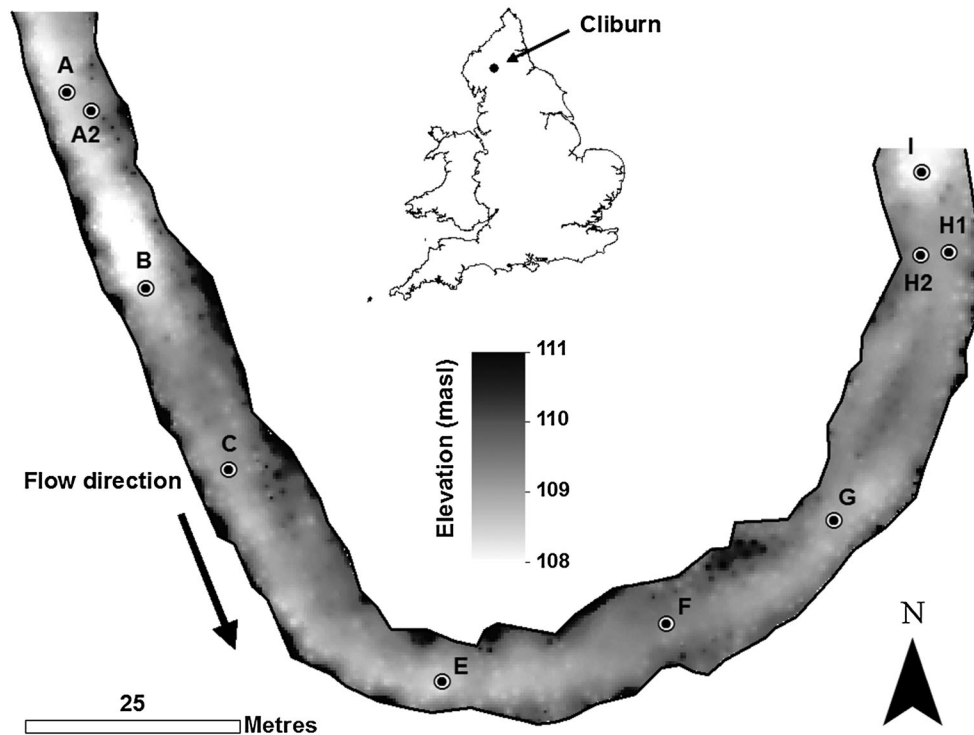


Figure 1. River Leith study reach showing riverbed elevation and the location of experimental sample sites

days equate to  $\sim Q_{90}$  ( $0.09 \text{ m}^3/\text{s}$ ) and  $\sim Q_{70}$  ( $1.31 \text{ m}^3/\text{s}$ ), respectively, from an examination of long-term discharge records (2004–2011).

**Piezometers.** As part of the wider parent project, a total of 88 PVCu piezometers were installed in the study reach in June 2009 and June 2010 in channel and riparian locations (Binley *et al.*, [submitted for review](#)). Channel piezometers were installed in nests; each piezometer nest consisting of three piezometers screened at 100, 50 and 20 cm below the riverbed. The present study is focused on eight piezometer nests covering the entire study reach (200 m) and encompassing both pools and riffles (Figure 1). Each 100-cm piezometer is fitted with multilevel pore water samplers at 10, 20, 50, and 100-cm depths. Pressure transducers logging the piezometer hydraulic head below the riverbed were installed at five sites (sites A, C, E, H2 and I) along the study reach (Figure 1).

**Hydrological measurements.** Manual (dip) measurements of the hydraulic head at each piezometer were taken using a graduated electrical contact dip metre. Dip measurements were taken at the same time as pore water samples to allow comparison between the hydrological and chemical datasets. Vertical hydraulic gradients (VHG) were calculated using  $dh/dl$ , with  $dh$  being the elevation difference between the piezometer water level and the stream level adjacent to the piezometer, and  $dl$  being the distance between the

midscreen depth of the piezometer and the riverbed surface. The vertical flux was calculated using Darcy's Law as  $q_v = K * dh/dl$ , where  $K$  is the hydraulic conductivity calculated from slug tests in the same piezometers used to compute hydraulic gradients (Binley *et al.*, [submitted for review](#)). Vertical flux based on the 100-cm depth head gradient uses the harmonic mean of  $K$  at 100, 50 and 20-cm depth. Vertical flux based on the 50-cm head gradient uses harmonic mean of  $K$  at 50 and 20 cm depth, whereas vertical flux based on the 20-cm depth head gradient uses  $K$  measured at 20-cm depth only. Pressure transducers at each site were used to record the river stage and the piezometer hydraulic head at 100 cm at 15-min intervals. Water levels were calibrated with discrete measurements after which the residual error between logged and dipped data was estimated at  $\pm 1.4 \text{ cm}$ .

**Pore water chemistry.** Prior to use, all plastic and glassware to be used in the field were acid washed in a laboratory. Pore water samples (40 ml) were collected from the multilevel samplers at 10, 20, 50 and 100-cm depths on each sample occasion. Samples were extracted using a syringe and flexible plastic tubing. Pore water sampling lines and syringes were flushed with pore water before collection of samples. A sample of the surface water near the piezometers was taken at the same time as pore water samples. All sample bottles were rinsed with pore water three times before sample collection, and samples were filtered ( $0.45 \mu\text{m}$  surfactant-free cellulose acetate membrane) in the

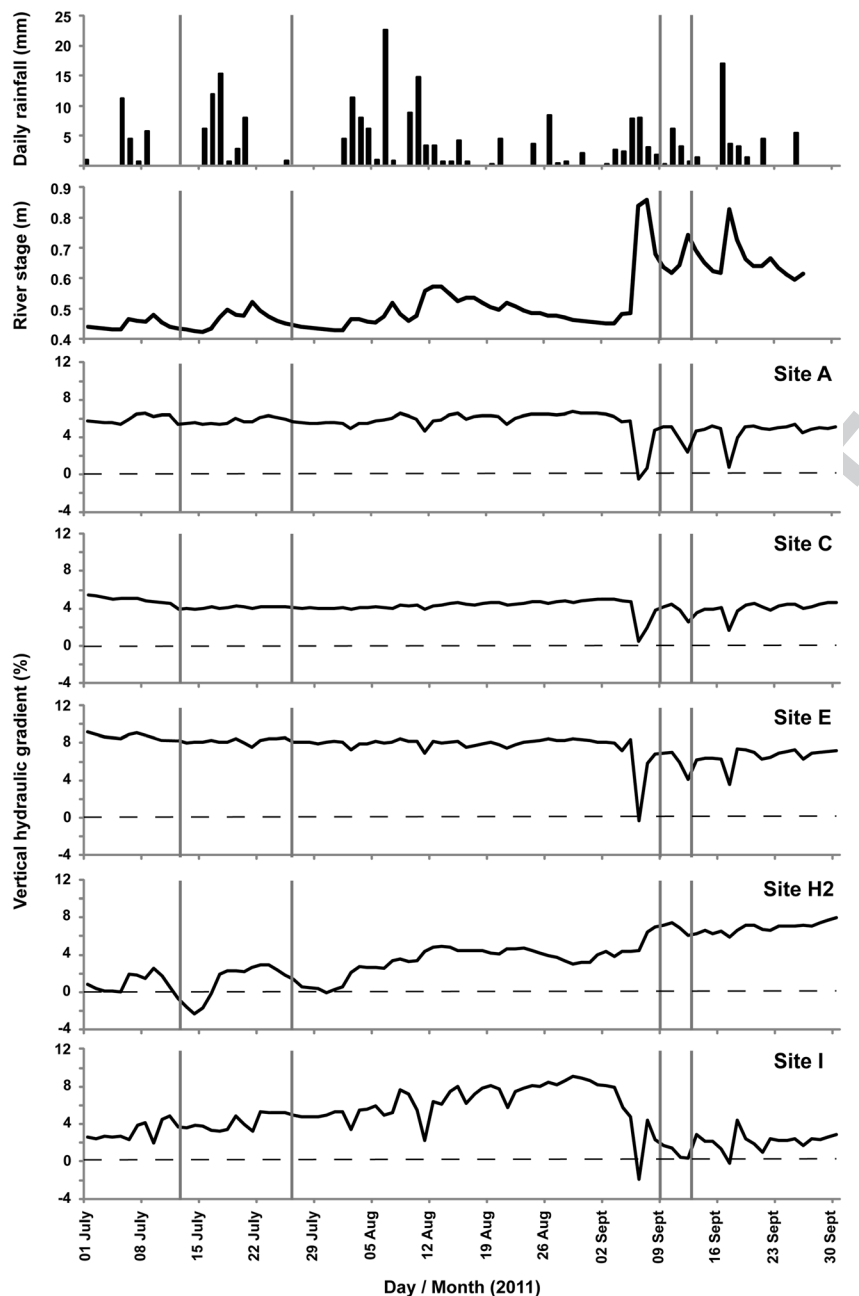


Figure 2. Daily rainfall, mean daily river stage and vertical hydraulic gradient (%) from logging pressure transducers at sites A, C, E, H2 and I for the study period. Sampling dates are indicated by the grey vertical lines. Horizontal dashed lines indicate zero vertical hydraulic gradient

field. Samples for ion ( $\text{NO}_3^-$ ,  $\text{NH}_4^+$ ,  $\text{SO}_4^{2-}$ ,  $\text{Cl}^-$ ) analysis were collected in polycarbonate bottles. Sample bottles were filled completely with sample water to avoid the presence of air pockets. Samples for Mn analysis were collected in 1.5 ml tubes and acidified with 20  $\mu\text{l}$  of 2 M HCl. Samples for DOC analysis were collected in amber glass bottles. Sample bottles were rinsed with pore water three times before adding the sample and acidifying to 2% HCl. All samples were transferred on ice to the laboratory within 4 h of collection and analysed within 24 h of

collection. On each sample occasion, two filter blanks were collected for all analytes.

**Laboratory analysis.** Nitrate,  $\text{SO}_4^{2-}$  and  $\text{Cl}^-$  were measured using ion chromatography (DIONEX), whereas  $\text{NH}_4^+$  was analyzed colorimetrically (seal AQ2 colorimetric analyzer using an adapted indophenol blue). The limit of detection across four separate analyses was 0.005 mg N/l  $\text{NO}_3^-$ , 0.14 mg/l  $\text{SO}_4^{2-}$ , 0.03 mg/l  $\text{Cl}^-$  and 0.008 mg N/l  $\text{NH}_4^+$ . The analytical precision was  $\pm 5.2\%$  for  $\text{NO}_3^-$ ,



$\pm 2.7\%$  for  $\text{SO}_4^{2-}$ ,  $\pm 1.7\%$  for  $\text{Cl}^-$  and  $\pm 3.8\%$  for  $\text{NH}_4^+$ . Manganese samples were measured using inductively coupled plasma-mass spectrometry (Thermo X series). DOC samples were measured using thermal oxidation (Thermalox TOC/TN analyser) by using the nonpurgeable organic carbon method. The limits of detection were  $0.09 \mu\text{g/l}$  Mn and  $0.58 \text{ mg/l}$  DOC. The analytical precision was  $\pm 3.6\%$  for Mn and  $\pm 6.3\%$  for DOC.

**Statistical data analysis.** One-way ANOVA was used to test for significant differences in environmental variables between sample depths (surface water and pore water at 10, 20, 50 and 100 cm). Where the data failed to comply with the normality of distribution assumption, the nonparametric equivalent (Kolmogorov–Smirnov test – nonparametric ANOVA) was used. Where significant differences occurred, the nonparametric Mann Whitney *U* test was used for pairwise comparison of surface water, shallow pore water (10 and 20 cm), deep pore water (50 and 100 cm), sample locations (riffles and pools) and stage levels (low, high).

The hydrological and chemical datasets were investigated further by using principal component analysis (PCA), a multivariate statistical analysis. Analyses were performed in the program CANOCO 4.5 (Ter Braak and Smilauer, 2002). Environmental data were  $\log_{10}(x+1)$  transformed before analysis to reduce the clustering of common and abundant measurements at the centre of the ordination plot and also the effect of outliers. Samples were centred and standardized by response (i.e. environmental) variables and scaling was focussed on response variables.

## RESULTS

### *Spatio-temporal patterns in subsurface hydrology and pore water chemistry*

**Subsurface hydrology.** The river stage for the study period gradually increased due to antecedent rainfall culminating in a series of high stage events in mid-September (Figure 2). There was a clear distinction in vertical hydraulic gradients between sample sites located in the upper (sites A, C and E) and lower (sites H2 and I) sections of the study reach. In the upper section, VHGs were relatively stable and positive throughout the study period until a series of high stage events in early September. These events coincided with a decrease in VHG at all three sample sites; a negative gradient was recorded at sites A and E during peak river stage on 8th September. Following the high stage events, the VHG returned to pre-event values from mid-September onwards. The vertical hydraulic gradients at sites H2 and I in the lower section of the study reach were mostly positive throughout the study period. At site H2, VHG increased with river stage ( $r = 0.91$ ;  $p = < 0.01$ ) apart from a period of approximately

6 days in mid-July when the gradient was negative. The VHG at site I deviated from this positive trend in response to the high stage events in September, exhibiting a dramatic reduction (and negative gradient) and similar characteristic response to sites in the upper section of the river. Due to the difficulty of sampling during high stage in the river, water sampling campaigns at high stage coincided with the falling limb of high flow events and not peak flow when VHG generally exhibited the most significant change in direction and magnitude (site A,  $6.6\%$  to  $-0.4\%$ ; site I,  $8.2\%$  to  $-1.9\%$ ).

The VHG-derived flux, calculated using Darcy's Law, exhibited spatial (depth and location) variability. Considering aggregated data (July and September sample dates) for the study reach, the mean vertical flux increased from 100 cm towards the riverbed (Table I), and values at 20 cm were significantly greater ( $p = < 0.01$ ) than those at 50 and 100 cm, which were more similar. This vertical trend persists when the sample sites are differentiated as pool (sites A, B, D and I) and riffle (sites C, F, G and H) sites (data not shown). Although mean values are larger at all three sample depths at riffle sites, no significant difference in vertical flux was found between pool and riffle sites.

No significant difference was recorded in aggregated vertical flux measurements between low and high stage

Table I. Mean and standard deviation (in parenthesis) of surface and pore water solutes (mg/L) and vertical flux measurements (m/day) in relation to sample depth and stage level

	Sample depth	<i>n</i>	Low stage	High stage
Vertical flux	20 cm	12	0.12 (0.10)	0.24 (0.29)
	50 cm	14	0.07 (0.13)	0.09 (0.13)
	100 cm	16	0.06 (0.07)	0.06 (0.05)
DOC	SW	16	3.0 (1.0)	5.2 (2.1)
	SPW	32	2.1 (1.7)	3.1 (2.1)
	DPW	32	1.3 (1.7)	2.8 (4.7)
Nitrate-N	SW	16	1.9 (0.2)	2.4 (0.1)
	SPW	32	3.9 (2.8)	3.7 (2.5)
	DPW	32	4.3 (2.7)	4.7 (2.6)
Ammonium-N	SW	16	0.03 (0.04)	0.03 (0.01)
	SPW	32	0.14 (0.32)	0.06 (0.14)
	DPW	32	0.01 (0.01)	0.02 (0.02)
Chloride	SW	16	27.7 (2.7)	16.7 (0.7)
	SPW	32	20.0 (4.8)	17.2 (1.7)
	DPW	32	16.9 (2.2)	17.1 (2.39)
Sulphate-S	SW	16	14.3 (1.4)	6.2 (0.9)
	SPW	32	8.7 (4.2)	6.6 (1.5)
	DPW	32	6.7 (2.0)	6.8 (2.1)
Manganese	SW	16	0.65 (1.16)	6.4 (3.0)
	SPW	32	0.55 (1.36)	122.4 (335.0)
	DPW	32	0.01 (0.04)	6.0 (17.5)

SW, surface water; SPW, shallow pore waters at 10 and 20 cm; DPW, deep pore waters at 50 and 100 cm; DOC, dissolved organic carbon

periods. However, closer examination of the relationship between low stage and high stage measurements reveals reach scale variation in vertical flux at 20-cm depth, which is not evident for deeper samples at 50 and 100 cm (Figure 3). An increase in vertical flux (20 cm) at high stage is found at three sample sites (sites F, G and H1) in the lower section of the study reach, while vertical flux (20 cm) decreases at high stage at two sites (sites B and C) in the upper section.

**Pore water chemistry.** Vertical profiles of pore water solutes ( $\text{Cl}^-$ ,  $\text{NO}_3^-$ , Mn and DOC) at low and high stage are presented in Figures 4 and 5 and explored further in scatterplots in Figure 6. Ammonium concentrations are not shown as values were generally below detection limits, and there were no significant differences found in concentrations between sample locations or stage levels. We also exclude  $\text{SO}_4^{2-}$  concentrations here as this solute was found to behave conservatively during the study period, exhibiting a strong correlation ( $r^2 = 0.614$ ;  $p = < 0.01$ ) with  $\text{Cl}^-$ . Lansdown *et al.* (2009) observed a similar conservative behaviour of  $\text{SO}_4^{2-}$  in our study reach during the 2009 and 2010 baseflow periods.

Chloride concentration profiles are used here as a tracer of surface–subsurface water interaction (Triska *et al.*, 1989; Hendricks and White, 1991). At the reach scale and at low stage, surface water  $\text{Cl}^-$  concentrations were significantly higher ( $p = < 0.01$ ) than pore water concentrations that were highest in the shallow sediments (10 and 20 cm) (Table I). Considering data from individual piezometers, surface–subsurface water mixing (based on  $\text{Cl}^-$  concentration profiles) did not appear to occur below 10 cm at most sample sites (Figure 4). However, notable exceptions were sites F and I where the approximate mixing depth occurred

at 10–20 and 20–50 cm, respectively. At sites G and H1, elevated  $\text{Cl}^-$  concentrations below 10 cm violate the assumption of simple surface water–groundwater mixing and suggest a third source of water was influencing the  $\text{Cl}^-$  profile at these sites. At high stage, there was a significant decrease ( $p = < 0.01$ ) in surface water  $\text{Cl}^-$  throughout the reach. At most sites this resulted in surface and pore water  $\text{Cl}^-$  concentrations becoming indistinguishable from each other (Table I). However, some sites (B and C) exhibited decreases in  $\text{Cl}^-$  concentration in shallow pore waters (Figure 6a) suggesting that mixing of surface and subsurface waters occurred below 10 cm (10–20 cm) at high stage. At site H1, elevated  $\text{Cl}^-$  persisted below 10 cm despite the decrease in surface water concentrations, suggesting the third source of water is important at this site at low and high stage.

Pore water  $\text{NO}_3^-$  concentrations at low and high stage exhibited a general longitudinal trend of decreasing values downstream in the study reach (with the exception of site I that was more characteristic of pore waters in the upper reach) (Figures 5a and 6b). At low and high stage, sites B, G, H1 and I had characteristic decreases in  $\text{NO}_3^-$  concentrations in the shallow sediments (10–20 cm); although the decrease was larger at high stage at site B,  $\text{NO}_3^-$  also decreased in the shallow sediments at high stage at site C. The  $\text{NO}_3^-$  profile at site G stands apart from the other sites where  $\text{NO}_3^-$  concentrations in the shallow sediments were lower than in deeper sediments and in the surface water. At site G,  $\text{NO}_3^-$  concentrations in the shallow sediments represented the lowest concentrations (0.10–0.43 mg N/l) recorded during the study period. Apart from the noted exceptions where  $\text{NO}_3^-$  decreased at high stage, an interesting occurrence was the generally higher surface and pore water  $\text{NO}_3^-$  concentrations at high stage (Table I, and Figures 5a and 6b).

Manganese concentrations in surface and pore waters were generally low (mostly below 0.1 mg/l) throughout the study period (Figure 5b) and, at low stage, were either below or very near to instrument detection limits (Table I). However, at high stage, there was a significant increase ( $p = < 0.01$ ) in Mn concentrations in surface and shallow (10 and 20 cm) pore waters (Figure 6c). At most sites, surface water Mn concentrations were higher than in the shallow sediments; however, at sites C, G (note change in abscissa scale) and I, Mn concentrations at either 10 or 20 cm were higher than in the surface water.

At low stage, DOC concentrations were higher in surface water than in pore waters (Table I and Figure 5c). For most sample sites, DOC concentrations were similar between shallow and deeper pore waters, although shallow pore water concentrations at sites G and I were higher than in deeper pore waters. At high stage, DOC concentrations increased at most sample sites in surface water and shallow pore waters in a similar manner to that

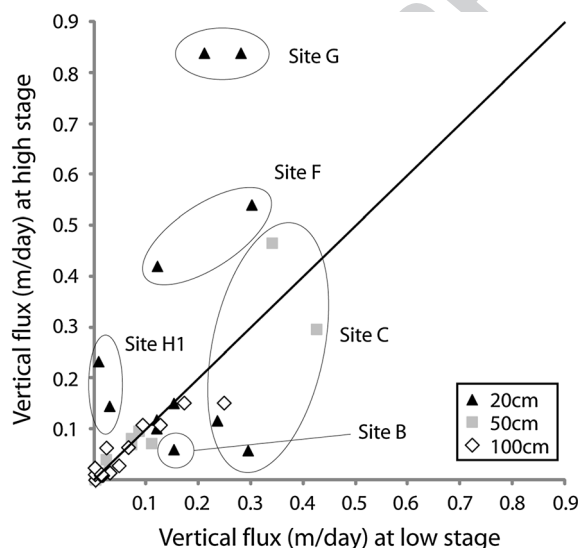


Figure 3. Scatterplot of all vertical flux measurements during low-stage and high-stage sampling periods

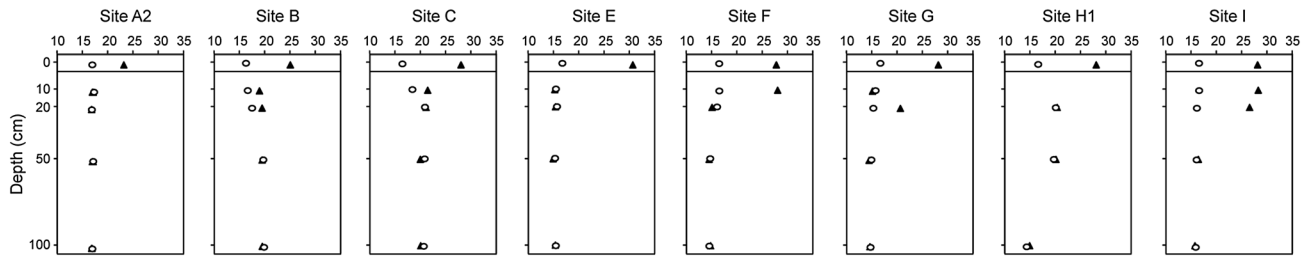


Figure 4. Summary of  $\text{Cl}^-$  [mean ( $n=2$ )] surface and pore water concentrations at all sample sites at low stage (triangles) and high stage (circles)

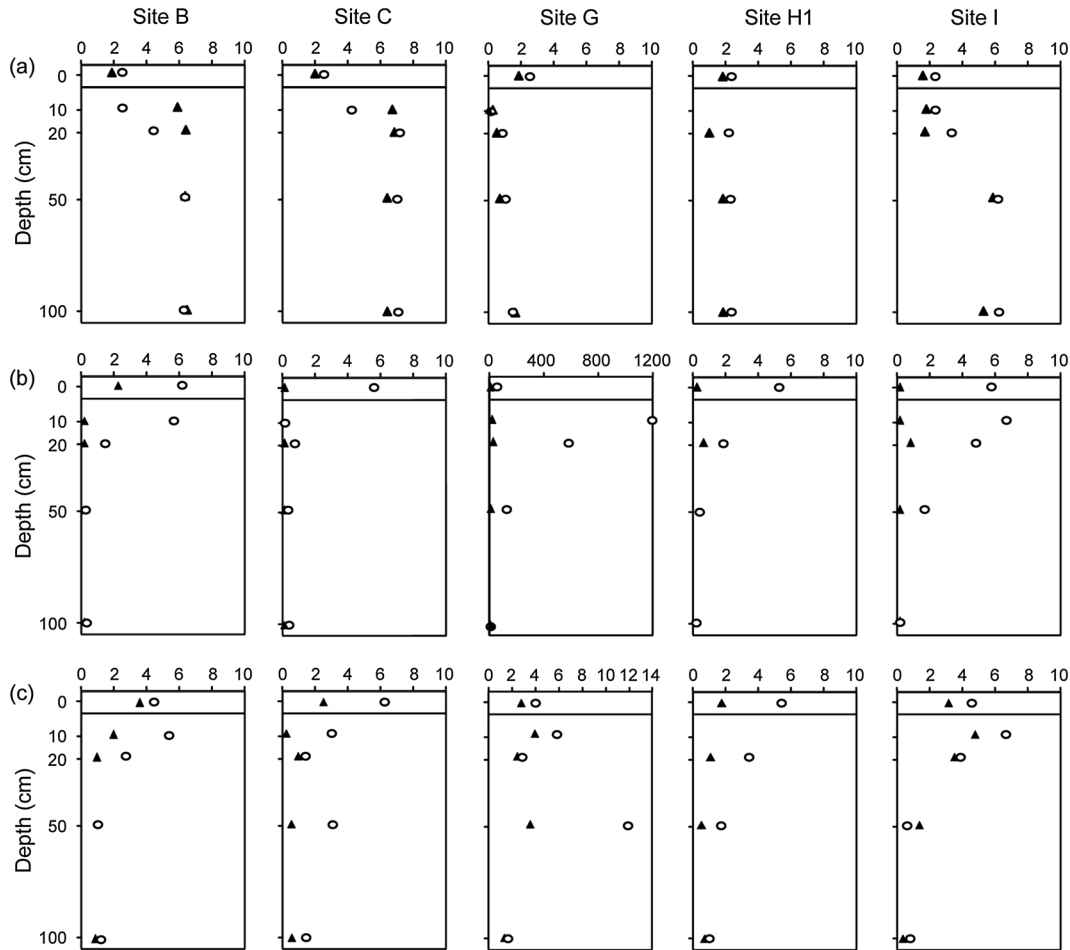


Figure 5. Summary of (a)  $\text{NO}_3^-$ , (b) Mn and (c) DOC [mean ( $n=2$ )] surface and pore water concentrations at sites B, C, G, H1 and I at low stage (triangles) and high stage (circles). Note different abscissa scale for DOC and Mn at site G

observed for Mn (Figure 6d). A number of sites exhibited higher DOC concentrations in pore water than surface water and/or abrupt increases in DOC at depth (sites B, C, G and I).

#### Principal component analysis of hydrological and chemical data

The previous sections have identified apparent changes in patterns of redox-sensitive solutes and in the depth of

hydraulic exchange associated with fluctuations in the river stage level. PCA is used in this section to identify the underlying factors explaining these changes in the environmental data. PCA is used in this study as many of the hydrological and chemical variables (factors) are correlated and the pattern of these correlations is consistent between sample periods. Preliminary PCA of the separate low and high stage datasets included the hydrological and chemical variables recorded at 20, 50 and 100-cm depths only. Chemical samples from surface

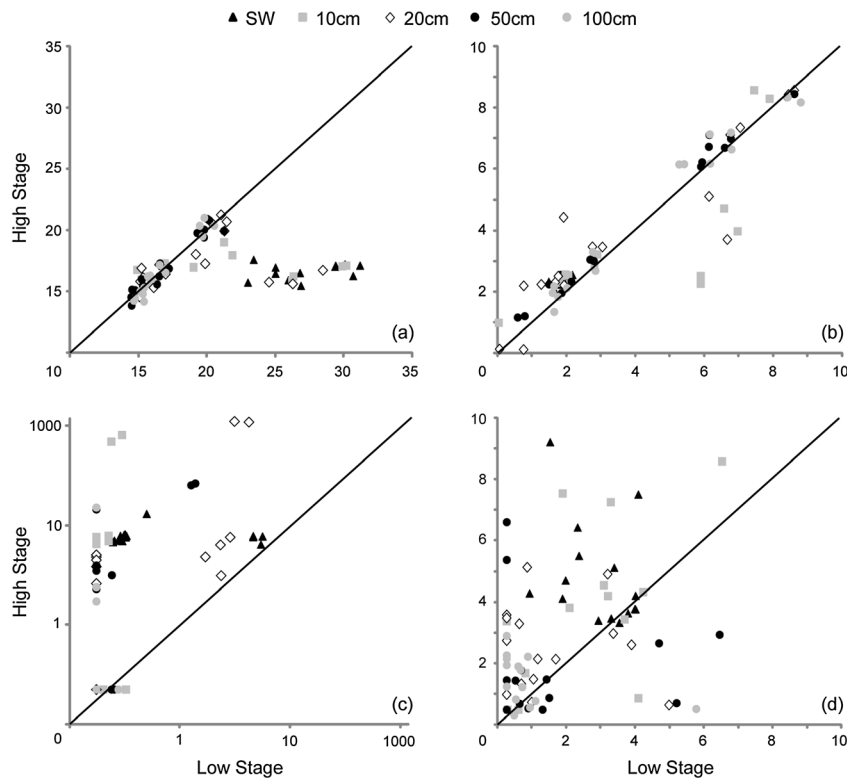


Figure 6. Scatterplots of (a)  $\text{Cl}^-$ , (b)  $\text{NO}_3^-$ , (c) Mn and (d) dissolved organic carbon surface and pore water concentrations during low and high stage sampling periods. SW, surface water sample

water and 10-cm depth were excluded from this first PCA as no comparable hydrological data existed. Results from this preliminary analysis indicated that vertical flux was not important in explaining variance in the datasets and was poorly correlated with the principal component axes. Therefore, a second PCA excluded vertical flux and included chemical data from surface water, 10, 20, 50 and 100-cm samples. The inclusion of surface water and pore water samples in this second analysis allowed for the potential discrimination of water source.

In the second PCA of chemical data at low river stage (run 1), the first two principal components explained 78.9% of the observed data variance and were therefore considered sufficient to explain any underlying environmental gradients (Table II). The first principal component (PC1) explained 48.6% of the observed data variance and was strongly and significantly correlated with all of the factors ( $\text{DOC}$ ,  $\text{NO}_3^-$ ,  $\text{NH}_4^+$ ,  $\text{SO}_4^{2-}$  and Mn) except  $\text{Cl}^-$ . The second principal component (PC2) accounted for a further 30.3% of the data variance and again exhibited strong correlations with the majority of factors. Figure 7 illustrates the ordination biplot for run 1 with samples labelled according to location (Figure 7a) and depth (Figure 7b). In the ordination biplots, factor gradients are represented by vectors and individual solute samples by points. Factors with long vectors explain more of the data variance than those with short vectors. Samples located

close to vectors are strongly associated with that vector and vice versa for samples projected near or beyond the origin of the vector. The samples are projected onto each vector with the order of projection corresponding to the ranking of the weighted averages of the samples with respect to the concentration of the factor. It is clear from the factor loadings on each principal component that there exist a number of chemical gradients in the study reach under low stage conditions. A large proportion of the samples are associated with the  $\text{NO}_3^-$  vector (Figure 7a), and closer inspection of the placement of these samples along the vector reveals the effect of sample location; there is an orderly progression of sample sites towards the vector origin reflecting movement downstream in the study reach. The vast majority of these samples are identified as 50 and 100-cm samples (Figure 7b) suggesting this locational influence is restricted primarily to these depths. Two further gradients are apparent in the low stage data, the first characterized principally by Mn and  $\text{NH}_4^+$  and the second by  $\text{SO}_4^{2-}$  and  $\text{Cl}^-$ . In addition, both of these gradients share an association with DOC. It is interesting that the majority of surface water, 10 and 20-cm samples are associated with one or the other of these two gradients suggesting changes in pore water chemistry are restricted primarily to these depths. Sites H1 and I exhibit a strong association with the  $\text{Cl}^-$  and  $\text{SO}_4^{2-}$  (and DOC) gradient, whereas sites C and G have strong associations with the Mn and  $\text{NH}_4^+$  (and DOC) gradient.



Table II. Principal component loadings and explained variance for the principal component analyses of chemical data. Correlations reported are the correlations between the principal components and the individual variables in the original dataset

	PC1 loadings	<i>r</i>	PC2 loadings	<i>r</i>
Run 1: low stage				
DOC	0.590	0.368**	-0.531	-0.721**
Nitrate-N	-0.666	-0.845**	0.710	0.727**
Ammonium-N	0.714	0.402**	0.557	-0.541**
Chloride	-0.573	-0.184	-0.581	-0.446**
Sulphate-S	-0.712	-0.294*	-0.484	-0.412**
Manganese	0.887	0.575**	0.222	-0.721**
% variance explained	48.6		30.3	
% cumulative variance	48.6		78.9	
Run 2: high stage				
DOC	0.083	0.636**	0.986	0.789**
Nitrate-N	-0.921	-0.644**	-0.304	-0.454**
Ammonium-N	-0.502	-0.493**	0.072	-0.055
Chloride	-0.715	-0.220	-0.170	-0.238*
Sulphate-S	-0.911	-0.441**	-0.327	-0.516**
Manganese	0.995	0.951**	-0.103	0.111
% variance explained	81.7		10.9	
% cumulative variance	81.7		92.6	

DOC, dissolved organic carbon

\*\*significant at 0.01 level;

\*significant at 0.05 level

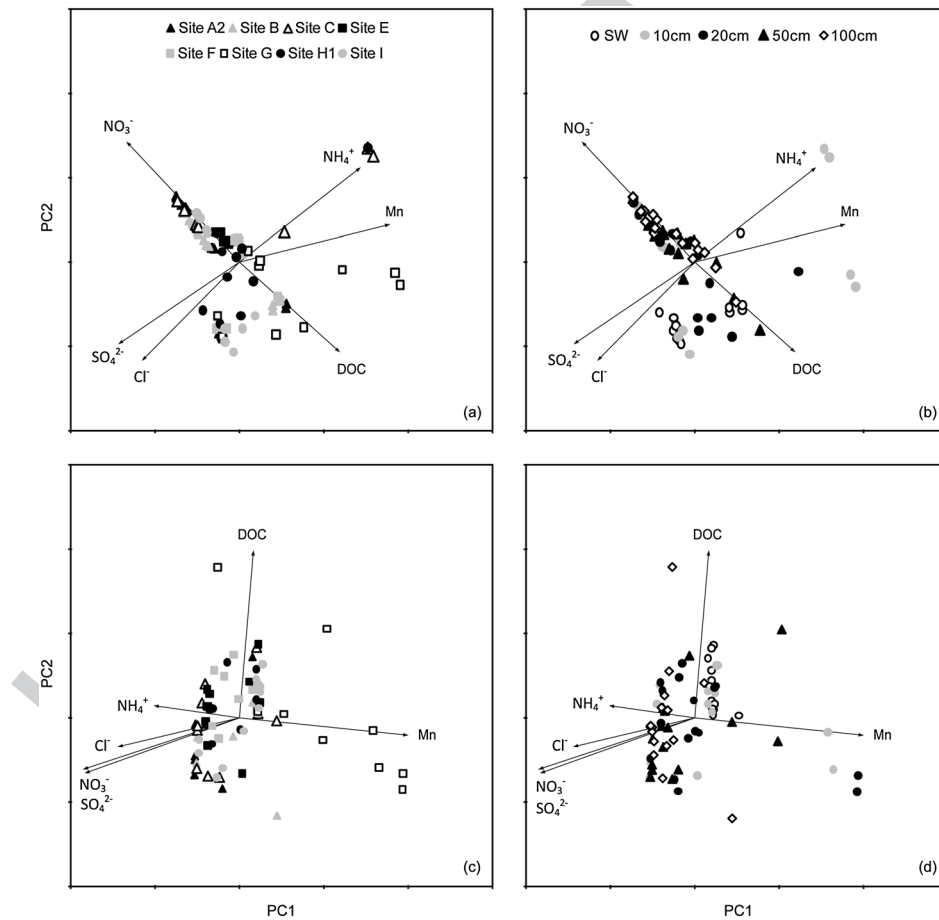


Figure 7. Principal component analysis biplots showing the distribution of surface and pore water chemical samples along the first two ordination axes for low-stage (a, b) and high-stage (c, d) sampling periods

Principal component analysis of the chemical data at high river stage (run 2) reveals a modification to the dominant environmental gradients identified in run 1. On this occasion, PC1 explains the majority of the variance in the dataset (81.7%) with PC2 only of minor importance (10.9%) (Table II). The first principal component is positively correlated with Mn and negatively with  $\text{NO}_3^-$ ,  $\text{NH}_4^+$ ,  $\text{Cl}^-$  and  $\text{SO}_4^{2-}$ . The second minor principal component is correlated most strongly with DOC. Examination of the PCA biplot identifies two linear sample clusters, the first associated with  $\text{NO}_3^-$ ,  $\text{NH}_4^+$ ,  $\text{Cl}^-$  and  $\text{SO}_4^{2-}$  and the second with Mn (Figure 7c). A number of separate samples (from site G) are strongly associated with the DOC and Mn gradients. The two linear sample clusters are also differentiated on the basis of sample depth (Figure 7d). The first sample cluster, associated with  $\text{NO}_3^-$ ,  $\text{NH}_4^+$ ,  $\text{Cl}^-$  and  $\text{SO}_4^{2-}$  are almost exclusively from 20, 50 and 100-cm depths, whereas the second cluster, associated with Mn, is composed principally of surface water and 10-cm samples. The samples most strongly associated with Mn are from 10 and 20-cm depths, and two samples associated with the DOC gradient are from 50 and 100-cm depths.

## DISCUSSION

### *Response of surface–subsurface hydraulic exchange to river stage variability*

Previously, Binley *et al.* (submitted for review) identified that vertical flux under baseflow conditions in our study reach was higher in the near-surface bed sediments (up to 20 cm) than that in deeper sediments. The present study has corroborated this finding. In addition, our results reveal significant changes in vertical flux at a 20-cm depth under high river stage conditions, although we emphasize that our results are based on a limited number of observations. At most downstream sites in the study reach (sites F, G and H1) vertical flux increased at high river stage. However, the reverse was true for some upstream sites (sites B and C). Other sites (sites A2, E and I) did not exhibit changes in vertical flux at this depth. Previous work on this stretch of river investigating spatial and temporal patterns of hyporheic flow has shown similar increases in VHGs associated with high stage events in part of the downstream reach (site F) (Käser *et al.*, 2009). This differential response in vertical flux between upstream and downstream sites may be related to the hydro-geomorphological characteristics of the two subreaches (Binley *et al.*, submitted for review). The river upstream of site E is deeply incised and constrained and can lead to river stage rising at a faster rate than groundwater hydraulic head; the steep-sided banks create a ‘bathtub’ from which water cannot escape

easily. This can result in weakening or reversal of the hydraulic gradient at high stage allowing surface water to enter the riverbed (see Figure 2). Downstream of site E, the river is typically less constrained with gently sloping banks (site I, a pool, is an exception and exhibits similar geomorphology to the upstream sites). At site H1, this allows water to overspill onto the floodplain at high stage, which maintains a positive hydraulic gradient in all but the highest stage events. At site I (a pool), the hydraulic gradient exhibits a similar trend to site H1 up to a critical point when the gradient decreases significantly and becomes negative. Käser *et al.* (2009) observed similar behaviour of vertical hydraulic gradients at sites H1 and I at low and high river stage.

By using end member mixing analysis of pore water data collected from our study reach, Lansdown *et al.* (submitted for review) have demonstrated that the proportion of infiltrating surface water in pore water may be different in pool and riffle environments. Our findings agree with this contention. At low stage at upstream sites (sites A2, B, C and E), surface–subsurface water mixing inferred from pore water  $\text{Cl}^-$  profiles does not appear to occur below 10 cm, whereas at sites further downstream (sites F, H1 and I), the  $\text{Cl}^-$  profile suggests mixing may occur deeper than 10 cm. Variability in hydraulic head over the downstream riffle sites (sites F, G and H1) may create potential for stream water infiltration (Hester and Doyle, 2008; Wondzell *et al.*, 2009). As site I is a pool and not a riffle, the  $\text{Cl}^-$  profile at this site may be more reflective of water that has infiltrated at site H1 and is now exfiltrating at the tail end of the riffle (i.e. site I). In contrast, the hydro-geomorphological environment of the upstream pool sites probably limits hyporheic exchange that might occur in rough bed environments that induce pumping exchange (Worman *et al.*, 2002). Aside from the influence of macroform geomorphology, at this study site, the pressure exerted by subsurface flux at low stage is greater at upstream than downstream sites that likely limits the vertical extent of the mixing zone (Binley *et al.*, submitted for review; Lansdown *et al.*, submitted for review).

In this paper, the emphasis is on understanding the change in mixing depth of HEFs under high river stage conditions. The disturbance to vertical flux caused by high river stage is reflected in the  $\text{Cl}^-$  surface and pore water measurements. At high river stage, surface water  $\text{Cl}^-$  concentrations were much lower than at low stage, which we interpret as a result of dilution by increased surface water flow in the river. Weakening of the vertical hydraulic gradient (at 100 cm) at upstream sites is evident from the pressure transducer data. There is also a significant decrease in vertical flux at 20 cm at high stage at sites B and C. These hydrological changes might have been sufficient to allow surface water infiltration at these

sites below 10 cm. When subsurface flux is reduced, HEF can extend as a function of the geomorphological and hydrogeological conditions (Cardenas and Wilson, 2007) that, in this stretch of river, indicate a permeable environment (Binley *et al.*, submitted for review). In the downstream section at site H1, it appears that the vertical hydraulic gradient increased in strength as the subsurface head rose at a faster rate than that of the river stage. At sites G and H1, it appears that the extent of the mixing zone was unchanged from its low stage position. A possible alternative is that the lower extent of the mixing zone had migrated towards the riverbed, that is, the mixing depth had decreased. This may have been caused by the additional pressure exerted by the increase in the hydraulic gradient. However, because of the scale at which we measured pore water chemistry, this possibility cannot be verified.

#### *Response of pore water chemistry to river stage variability*

The PCA of the chemical samples from low stage sampling days revealed a strong longitudinal  $\text{NO}_3^-$  gradient within the study reach and generally higher anion concentrations in the pore waters of the upstream section of the river. This pore water gradient has also been observed by Binley *et al.* (submitted for review) who suggest the upper section of our study reach (centred on site C) may be a preferential discharge location (Conant, 2004) directly connected to the underlying bedrock. Heppell *et al.* (in prep) have further identified this zone as predominantly oxic and responsible for 4–9% of total  $\text{NO}_3^-$  transported through the reach in surface water under low stage conditions. The present study has observed this longitudinal trend in  $\text{NO}_3^-$  to be most significant in the deeper pore waters at 50 and 100-cm depths. The surface and shallow pore waters (10 and 20 cm) exhibited more chemical variability than the deeper pore waters. An important gradient identified by the PCA was that characterized by  $\text{SO}_4^{2-}$  and  $\text{Cl}^-$  that may reflect a different source of water to the upwelling subsurface water, which has lower  $\text{SO}_4^{2-}$  and  $\text{Cl}^-$  concentrations (Heppell *et al.*, in prep). Lansdown *et al.* (submitted for review) and Heppell *et al.* (in prep) have previously demonstrated the conservative nature of  $\text{SO}_4^{2-}$  and its similar behaviour to  $\text{Cl}^-$  in our study reach. This 'source' gradient may reflect shallow surface–subsurface water mixing (HEF) at sites F, G, H1 and I in the lower part of the study reach. Heppell *et al.* (in prep) have observed predominantly chemically reducing conditions in the pore waters of this downstream section of our study reach (sites G to I). Similarly, the present study identified a chemical signature (low  $\text{NO}_3^-$ ; elevated Mn and  $\text{NH}_4^+$ ) at sites G and H1 suggestive of a reduced environment. This chemical signature is most likely related

to aerobic respiration (Morrice *et al.*, 2000); however, Lansdown *et al.* (2012) found the bed sediments of our study reach to have low sediment-bound carbon. Several workers (Stelzer and Bartsch, 2012; Lansdown *et al.*, submitted for review) have suggested that organic material may be supplied to the subsurface from surface water or shallow lateral sources distinct from the point of sampling. In the present study, elevated DOC occurred below the hypothesized surface–subsurface water mixing depth at sites F, G and H1 suggesting a lateral flowing, DOC-rich, source of water may be influencing pore water chemistry at these sites. Binley *et al.* (submitted for review) confirm the importance of lateral subsurface flows from the riparian zone in this downstream section of our study reach. It is possible that the elevated DOC found at these sites is the result of the continuous supply of organic material along lateral subsurface flow paths linked to the riparian zone. An alternative hypothesis is that the elevated DOC found in the pore waters is a remnant of DOC-rich surface water and/or subsurface water delivered to the point of sampling as a result of changes in hydraulic gradients induced by the passage of a flood wave. This possibility is considered below by discussing changes in subsurface hydrology linked to chemical patterns.

The PCA of the high river stage dataset revealed a significant change in the pattern of surface and pore water chemistry observed at low stage. A single gradient explained the majority of the sample variance (81.7%) being characterized at one end by samples with high  $\text{NO}_3^-$ ,  $\text{SO}_4^{2-}$ ,  $\text{Cl}^-$  and  $\text{NH}_4^+$  and at the other end by samples with elevated Mn. A secondary gradient is associated with DOC. The large cluster of samples associated with high  $\text{NO}_3^-$ ,  $\text{SO}_4^{2-}$ ,  $\text{Cl}^-$  and  $\text{NH}_4^+$  perhaps represents the effect of location and on this occasion extends also to 20 cm; the result of increased flux at high stage reducing the depth of surface water infiltration at some sites. The second cluster of samples associated with the DOC and Mn vectors is made up primarily of surface water and 10-cm-depth samples and is characterized by low  $\text{NO}_3^-$ ,  $\text{SO}_4^{2-}$ ,  $\text{Cl}^-$  and  $\text{NH}_4^+$  (and high DOC and Mn) concentrations. The sites most associated with this cluster are G, H1 and I. The reason for the increase in DOC and Mn concentrations in surface water at high stage may be related primarily to erosion and runoff from the surrounding land (Heal *et al.*, 2002; Veum *et al.*, 2009) and, in the case of Mn, to the formation of colloidal complexes that are able to pass through the sample filter (Scott *et al.*, 2002).

We have noted previously that at low river stage, elevated DOC occurred below the hypothesized surface–groundwater mixing depth at sites F, G and H1. At high river stage, DOC concentrations increased in the pore waters as did vertical flux at 20 cm; together these occurrences suggest a lateral moving, DOC-rich source of

water is contributing to overall flux at these sites. This lateral moving water may derive from the low lying alluvial sediments of the riparian zone. Käser *et al.* (2009) have previously reported synchronous behaviour between subsurface heads and riparian heads in the same subreach as sites F, G and H1. They concluded that this was probably caused by a pressure wave propagating in the subsurface in response to a rise in river stage. It is well-known that subsurface transitory flow (Hewlett and Hibbert, 1967) associated with a fluid pressure wave can result in pre-event or 'old' water contributing significantly to runoff during a storm event. The relative contribution of transitory flow to the stormflow hydrograph is strongly linked to the saturation level of the soil (Hewlett and Hibbert, 1967). If the water content of the soil is near that required for fluid flow (near or above retention capacity), then only a relatively small volume of rainfall is required to transmit a wave of fluid pressure (almost instantaneously) through a soil system (Charbeneau, 1984). In the period between our low and high stage events a significant amount of rainfall fell on the catchment with only limited response in the river hydrograph (Figure 2). It is probable that elevated catchment wetness prior to the recorded high stage events resulted in the increased vertical flux (at 20-cm depth) observed at some sites. The mechanism may have been a corresponding increase in lateral flux caused by transitory flow from the riparian zone. This lateral flux would exert a pressure on the hyporheic flow system reducing the extent of the surface–subsurface water mixing zone. *The absence of such a mechanism in the upper part of the study reach is most likely related to the 'bathtub' geomorphology that restricts the movement of water from the riparian zone to the river channel.*

#### *Process drivers in the hyporheic zone at high river stage*

We propose the following general process drivers in our study reach that may account for the observed changes in pore water chemistry at high river stage. In the upper reach, vertical flux was reduced at some sites (sites B and C) at a 20-cm depth and did not change at 50 and 100-cm depths. The weakening of the vertical gradient in the upper sediments, combined with the permeable nature of these sediments, allowed hyporheic exchange flows to develop and to extend below 10 cm (approximately at a 10–20-cm depth). Down welling surface water with elevated DOC and colloidal Mn increased the concentrations of these solutes in the upper 20 cm of the riverbed. Nitrate in the upper sediments decreased possibly as a result of mixing with down welling low  $\text{NO}_3^-$  surface water. In the lower reach, vertical flux at a 20-cm depth increased significantly at some sites (sites F, G and H1) over low stage values because of contributions from lateral water sources, most

likely originating from the low lying alluvial sediments. This constrained the vertical (and probably lateral) extent of the hyporheic mixing zone, maintaining or possibly decreasing its depth. Elevated DOC and colloidal Mn were introduced to the shallow sediments (10-cm depth) by down welling surface water. Lateral moving reduced water from the alluvial sediments introduced DOC and Mn to deeper sediments (20–50 cm). At site G, highly elevated Mn in the shallow sediments suggests that *in situ* biogeochemical reduction might also be controlling the observed chemical pattern at this site. Dissolved oxygen measurements (data not shown) taken at low stage as part of the wider parent project, but not coinciding with the sampling dates of the present study, indicate site G to have consistently low oxygen saturation values at 10 and 20-cm depths (minimum 1% saturation) that generally increase (maximum 61% saturation) in deeper sediments at 100 cm. It is possible that the enhanced delivery of DOC (via lateral flows) to these low oxygen sediments during high river stage fuels biological reduction of both  $\text{NO}_3^-$  and Mn leading to the observed chemical patterns.

## CONCLUSIONS

We have found the river stage and the geomorphologic environment to be important drivers of chemical patterns in the hyporheic zone. Our hypothesis suggested that high river stage would cause upwelling flow paths in our study reach to weaken or reverse and this change would affect surface–subsurface water exchange and chemical patterns. A differential response in vertical flux between upper and lower sections of our study reach was most likely due to geomorphologic environment. At high stage, weakening of the vertical hydraulic gradient occurred in a generally constrained and deeply incised subreach. Strengthening of the vertical gradient occurred in a subreach with more gently sloping banks, probably as a result of the contribution of lateral subsurface flows from low lying alluvial sediments.

The different response in vertical flux between the two subreaches was reflected in the reactive chemistry of the hyporheic sediments. The weaker vertical hydraulic gradient in the constrained subreach appeared to allow hyporheic exchange flows to extend vertically and deliver reactive solutes to the upper sediments. Strengthening of the vertical hydraulic gradient in the more open subreach maintained or reduced the vertical extent of mixing. However, reactive solutes were still delivered deep into the hyporheic sediments. Down welling surface water was probably responsible for contributions to the shallow sediments where surface–subsurface water mixing still existed, whereas lateral subsurface flows were probably responsible for deeper contributions.



Conventional thinking might suggest high river flows, which cause oxygenated surface water to infiltrate into sediment might result in net gain of nutrients in surface water through processes such as ammonification and nitrification. Our research suggests this might not be the case and that the delivery of DOC to hyporheic sediments during high river stage may instead fuel biogeochemical reduction processes. This could be particularly important in a reach where, under predominant baseflow conditions, strong groundwater upwelling effectively constrains the spatial extent of the hyporheic zone and its ability to attenuate nutrients.

#### ACKNOWLEDGEMENTS

This work was supported by a Natural Environment Research Council grant awarded to Lancaster University (NE/F006063/1) and Queen Mary, University of London (NE/F004753/1). The Environment Agency of England and Wales is gratefully acknowledged for providing precipitation and river stage, and discharge data. We thank Lorna Meek, Amy Graham, Gareth McShane and Heather Carter for their valued assistance with field sampling and laboratory analyses.

#### REFERENCES

- Binley A, Ullah S, Heathwaite AL, Heppell CM, Byrne P, Lansdown K, Trimmer M, Zhang H. submitted for review. Revealing the spatial variability of water fluxes at the groundwater–surface water interface. *Water Resources Research*. [Q3]
- Boano F, Revelli R, Ridolfi L. 2011. Water and solute exchange through flat streambeds induced by large turbulent eddies. *Journal of Hydrology* **402**: 290–296. DOI: 10.1016/j.jhydrol.2011.03.023.
- Boulton AJ. 2007. Hyporheic rehabilitation in rivers: restoring vertical connectivity. *Freshwater Biology*, **52**: 632–650. DOI: 10.1111/j.1365-2427.2006.01710.x.
- Briggs MA, Lautz LK, McKenzie JM, Gordon RP, Hare DK. 2012. Using high-resolution distributed temperature sensing to quantify spatial and temporal variability in vertical hyporheic flux. *Water Resources Research* **48**. DOI: 10.1029/2011wr011227.
- Cardenas MB, Wilson JL. 2007. Exchange across a sediment–water interface with ambient groundwater discharge. *Journal of Hydrology* **346**: 69–80. DOI: 10.1016/j.jhydrol.2007.08.019.
- Charbeneau RJ. 1984. Kinematic models for soil–moisture and solute transport. *Water Resources Research* **20**: 699–706. DOI: 10.1029/WR020i006p00699.
- Conant B. 2004. Delineating and quantifying ground water discharge zones using streambed temperatures. *Ground Water* **42**: 243–257. DOI: 10.1111/j.1745-6584.2004.tb02671.x.
- Gu CH, Hornberger GM, Herman JS, Mills AL. 2008a. Effect of freshets on the flux of groundwater nitrate through streambed sediments. *Water Resources Research* **44**. DOI: 10.1029/2007wr006488.
- Gu G, Hornberger GM, Herman JS, Mills AL. 2008b. Influence of stream–groundwater interactions in the streambed sediments on  $\text{NO}_3^-$  flux to a low-relief coastal stream. *Water Resources Research* **44**: W11432. DOI: doi:10.1029/2007WR006739.
- Heal KV, Kneale PE, McDonald AT. 2002. Manganese in runoff from upland catchments: temporal patterns and controls on mobilization. *Hydrological Sciences Journal* **47**: 769–780. DOI: 10.1080/02626660209492979. [Q4]
- Hendricks SP, White DS. 1991. Physicochemical patterns within a hyporheic zone of a northern Michigan river, with comments on surface-water patterns. *Canadian Journal of Fisheries and Aquatic Sciences* **48**: 1645–1654. DOI: 10.1139/f91-195.
- Hester ET, Doyle MW. 2008. In-stream geomorphic structures as drivers of hyporheic exchange. *Water Resources Research* **44**. DOI: 10.1029/2006wr005810.
- Hewlett JD, Hibbert AR. 1967. Factors affecting the response of small watersheds to precipitation in humid areas. In: *Proceedings of the International Symposium on Forest Hydrology*, Sopper WE, Lull HW (eds.) Pergamon, New York; 275–290.
- Kasahara T, Wondzell SM. 2003. Geomorphic controls on hyporheic exchange flow in mountain streams. *Water Resources Research* **39**. DOI: 10.1029/2002wr001386.
- Käser DH, Binley A, Heathwaite AL, Krause S. 2009. Spatio-temporal variations of hyporheic flow in a riffle-step-pool sequence. *Hydrological Processes* **23**: 2138–2149. DOI: 10.1002/hyp.7317.
- Krause S, Heathwaite L, Binley A, Keenan P. 2009. Nitrate concentration changes at the groundwater–surface water interface of a small Cumbrian river. *Hydrological Processes* **23**: 2195–2211. DOI: 10.1002/hyp.7213.
- Lansdown K, Heppell CM, Binley A, Heathwaite AL, Ullah S, Byrne P, Zhang H, Heaton THE, Keenan P, Trimmer M. submitted for review. Quantifying reach-scale variability in surface water downwelling and its implications for hyporheic nitrate dynamics in the bed of a groundwater-fed river. *Journal of Hydrology*. [Q5]
- Lansdown K, Trimmer M, Heppell CM, Sgouridis F, Ullah S, Heathwaite AL, Binley A, Zhang H. 2012. Characterization of the key pathways of dissimilatory nitrate reduction and their response to complex organic substrates in hyporheic sediments. *Limnology and Oceanography* **57**: 387–400. DOI: 10.4319/lo.2012.57.2.0387.
- Lautz L, Fanelli R. 2008. Seasonal biogeochemical hotspots in the streambed around restoration structures. *Biogeochemistry* **91**: 85–104. DOI: 10.1007/s10533-008-9235-2.
- Morrice JA, Dahm CN, Valett HM, Unnikrishna PV, Campana ME. 2000. Terminal electron accepting processes in the alluvial sediments of a headwater stream. *Journal of the North American Benthological Society* **19**: 593–608. DOI: 10.2307/1468119.
- Mulholland PJ, Hall RO, Sobota DJ, Dodds WK, Findlay SEG, Grimm NB, Hamilton SK, McDowell WH, O'Brien JM, Tank JL, Ashkenas LR, Cooper LW, Dahm CN, Gregory SV, Johnson SL, Meyer JL, Peterson BJ, Poole GC, Valett HM, Webster JR, Arango CP, Beaulieu JJ, Bernot MJ, Burgin AJ, Crenshaw CL, Helton AM, Johnson LT, Niederlehner BR, Potter JD, Sheibley RW, Thomas SM. 2009. Nitrate removal in stream ecosystems measured by N-15 addition experiments: denitrification. *Limnology and Oceanography* **54**: 666–680. DOI: 10.4319/lo.2009.54.3.0666.
- Munz M, Krause S, Tecklenburg C, Binley A. 2011. Reducing monitoring gaps at the aquifer–river interface by modelling groundwater–surface water exchange flow patterns. *Hydrological Processes* **25**: 3547–3562. DOI: 10.1002/hyp.8080.
- Packman A, Salehin M, Zaramella M. 2004. Hyporheic exchange with gravel beds: basic hydrodynamic interactions and bedform-induced advective flows. *Journal of Hydraulic Engineering-Asce* **130**: 647–656. DOI: 10.1061/(asce)0733-9429(2004)130:7(647). [Q6]
- Rance J, Wade SD, Hurford AP, Bottius E, Reynard NS. 2012. Climate Change Risk Assessment for the Water Sector. Department for Environment, Food and Rural Affairs.
- Scott DT, McKnight DM, Voelker BM, Hrcir DC. 2002. Redox processes controlling manganese fate and transport in a mountain stream. *Environmental Science and Technology* **36**: 453–459. DOI: 10.1021/es010951s.
- Stelzer RS, Bartsch LA. 2012. Nitrate removal in deep sediments of a nitrogen-rich river network: a test of a conceptual model. *Journal of Geophysical Research-Biogeosciences* **117**. DOI: 10.1029/2012jg001990.
- Ter Braak CJF, Smilauer P. 2002. CANOCO Reference Manual and CanoDraw for Windows User's Guide: Software for Canonical Community Ordination (version 4.5). Microcomputer Power.
- Triska FJ, Kennedy VC, Avanzino RJ, Zellweger GW, Bencala KE. 1989. Retention and transport of nutrients in a 3rd-order stream in northwestern California – hyporheic processes. *Ecology* **70**: 1893–1905. DOI: 10.2307/1938120.

- Veum KS, Goynes KW, Motavalli PP, Udawatta RP. 2009. Runoff and dissolved organic carbon loss from a paired-watershed study of three adjacent agricultural watersheds. *Agriculture, Ecosystems & Environment* **130**: 115–122. DOI: 10.1016/j.agee.2008.12.006.
- Westhoff MC, Gooseff MN, Bogaard TA, Savenije HHG. 2011. Quantifying hyporheic exchange at high spatial resolution using natural temperature variations along a first-order stream. *Water Resources Research* **47**. DOI: 10.1029/2010wr009767.
- Wondzell SM, LaNier J, Haggerty R, Woodsmith RD, Edwards RT. 2009. Changes in hyporheic exchange flow following experimental wood removal in a small, low-gradient stream. *Water Resources Research* **45**. DOI: 10.1029/2008wr007214.
- Worman A, Packman AI, Johansson H, Jonsson K. 2002. Effect of flow-induced exchange in hyporheic zones on longitudinal transport of solutes in streams and rivers. *Water Resources Research* **38**. DOI: 10.1029/2001wr000769.
- Wroblicky GJ, Campana ME, Valett HM, Dahm CN. 1998. Seasonal variation in surface–subsurface water exchange and lateral hyporheic area of two stream-aquifer systems. *Water Resources Research* **34**: 317–328. DOI: 10.1029/97wr03385.
- Zarnetske JP, Haggerty R, Wondzell SM, Baker MA. 2011a. Dynamics of nitrate production and removal as a function of residence time in the hyporheic zone. *Journal of Geophysical Research-Biogeosciences* **116**. DOI: 10.1029/2010jg001356.
- Zarnetske JP, Haggerty R, Wondzell SM, Baker MA. 2011b. Labile dissolved organic carbon supply limits hyporheic denitrification. *Journal of Geophysical Research-Biogeosciences* **116**. DOI: 10.1029/2011jg001730.

# Author Query Form

---

**Journal: Hydrological Processes**

**Article: hyp\_9981**

Dear Author,

During the copyediting of your paper, the following queries arose. Please respond to these by annotating your proofs with the necessary changes/additions.

- If you intend to annotate your proof electronically, please refer to the E-annotation guidelines.
- If you intend to annotate your proof by means of hard-copy mark-up, please refer to the proof mark-up symbols guidelines. If manually writing corrections on your proof and returning it by fax, do not write too close to the edge of the paper. Please remember that illegible mark-ups may delay publication.

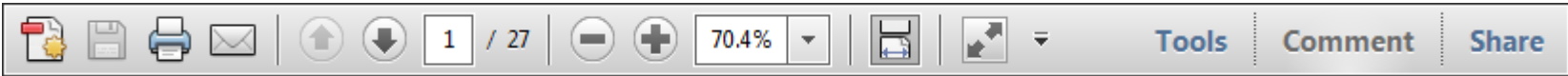
Whether you opt for hard-copy or electronic annotation of your proofs, we recommend that you provide additional clarification of answers to queries by entering your answers on the query sheet, in addition to the text mark-up.

Query No.	Query	Remark
Q1	AUTHOR: Please check the presentation of compass directions if acceptable or inconsistent. 'N54:37:03; W2:38:23' and '64:39:10E; 26:71:00 N.	
Q2	AUTHOR: Please give address information for all manufacturers captured in the body: town, state (if applicable), and country.	
Q3	AUTHOR: If this reference has now been published online, please add relevant year/DOI information. If this reference has now been published in print, please add relevant volume/issue/page/year information.	
Q4	AUTHOR: Original Hydrol. Sci. J.-J. Sci. Hydrol. was change to Hydrological Sciences Journal, please check if correct.	
Q5	AUTHOR: If this reference has now been published online, please add relevant year/DOI information. If this reference has now been published in print, please add relevant volume/issue/page/year information.	
Q6	AUTHOR: Reference "Packman et al. (2004)" is not cited in the text. Please indicate where it should be cited; or delete from the reference list.	

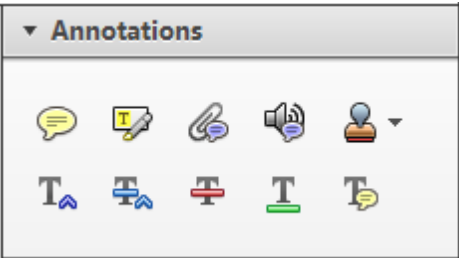
USING e-ANNOTATION TOOLS FOR ELECTRONIC PROOF CORRECTION

Required software to e-Annotate PDFs: Adobe Acrobat Professional or Adobe Reader (version 7.0 or above). (Note that this document uses screenshots from Adobe Reader X)  
The latest version of Acrobat Reader can be downloaded for free at: <http://get.adobe.com/uk/reader/>

Once you have Acrobat Reader open on your computer, click on the [Comment](#) tab at the right of the toolbar:



This will open up a panel down the right side of the document. The majority of tools you will use for annotating your proof will be in the [Annotations](#) section, pictured opposite. We've picked out some of these tools below:



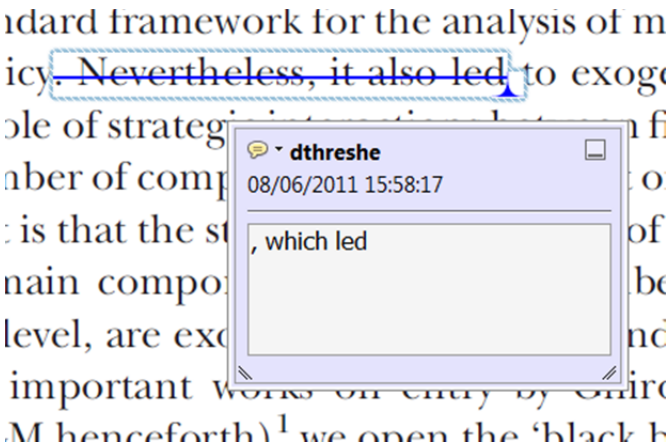
1. [Replace \(Ins\)](#) Tool – for replacing text.



Strikes a line through text and opens up a text box where replacement text can be entered.

How to use it

- Highlight a word or sentence.
- Click on the [Replace \(Ins\)](#) icon in the Annotations section.
- Type the replacement text into the blue box that appears.



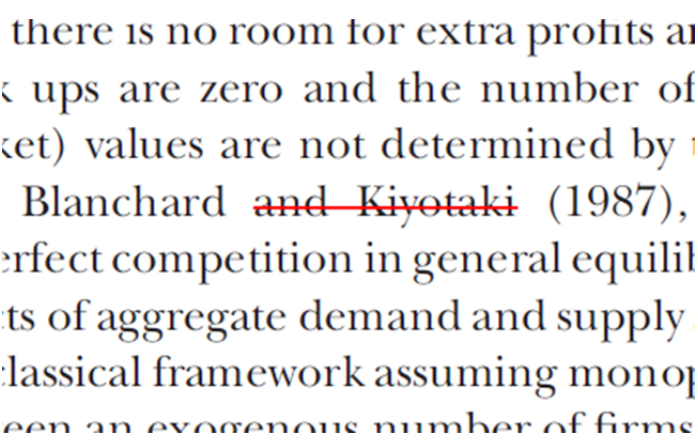
2. [Strikethrough \(Del\)](#) Tool – for deleting text.



Strikes a red line through text that is to be deleted.

How to use it

- Highlight a word or sentence.
- Click on the [Strikethrough \(Del\)](#) icon in the Annotations section.



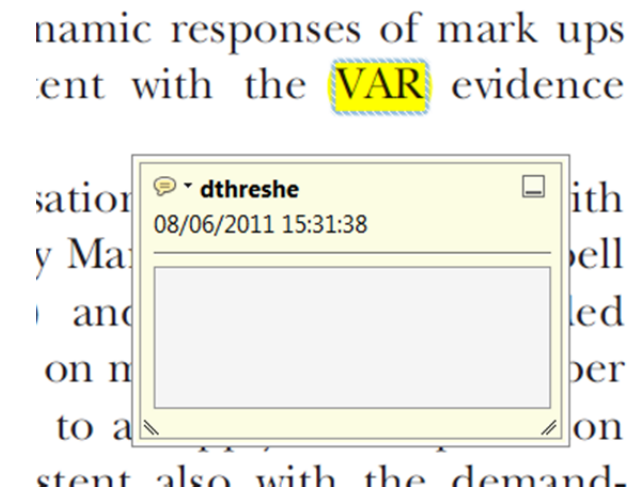
3. [Add note to text](#) Tool – for highlighting a section to be changed to bold or italic.



Highlights text in yellow and opens up a text box where comments can be entered.

How to use it

- Highlight the relevant section of text.
- Click on the [Add note to text](#) icon in the Annotations section.
- Type instruction on what should be changed regarding the text into the yellow box that appears.



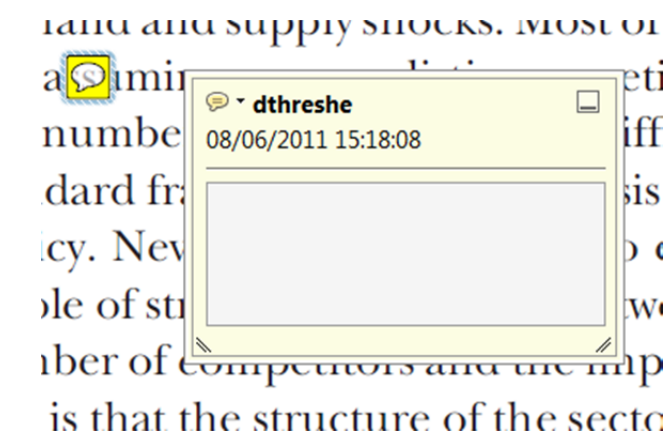
4. [Add sticky note](#) Tool – for making notes at specific points in the text.



Marks a point in the proof where a comment needs to be highlighted.

How to use it

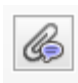
- Click on the [Add sticky note](#) icon in the Annotations section.
- Click at the point in the proof where the comment should be inserted.
- Type the comment into the yellow box that appears.





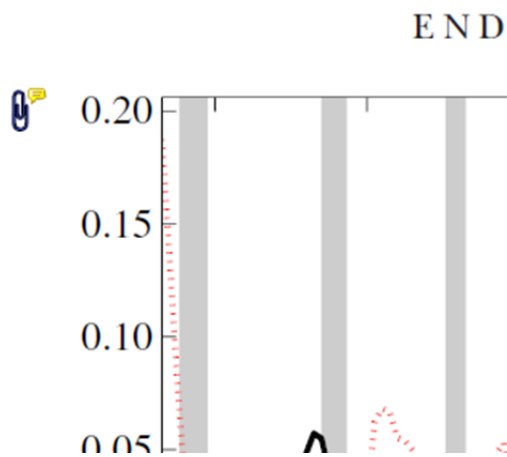
USING e-ANNOTATION TOOLS FOR ELECTRONIC PROOF CORRECTION

5. **Attach File** Tool – for inserting large amounts of text or replacement figures.


 Inserts an icon linking to the attached file in the appropriate place in the text.

How to use it

- Click on the **Attach File** icon in the Annotations section.
- Click on the proof to where you'd like the attached file to be linked.
- Select the file to be attached from your computer or network.
- Select the colour and type of icon that will appear in the proof. Click OK.



6. **Add stamp** Tool – for approving a proof if no corrections are required.

 Inserts a selected stamp onto an appropriate place in the proof.

How to use it

- Click on the **Add stamp** icon in the Annotations section.
- Select the stamp you want to use. (The **Approved** stamp is usually available directly in the menu that appears).
- Click on the proof where you'd like the stamp to appear. (Where a proof is to be approved as it is, this would normally be on the first page).

of the business cycle, starting with the  
on perfect competition, constant return  
production. In this environment goods  
extra profits and the structure of market  
he number of firms in the individual firm  
etermined by the model. The New-Key  
otaki (1987), has introduced product  
general equilibrium models with nomin  
ed and supply shocks. Most of this literat

**APPROVED**

Drawing Markups

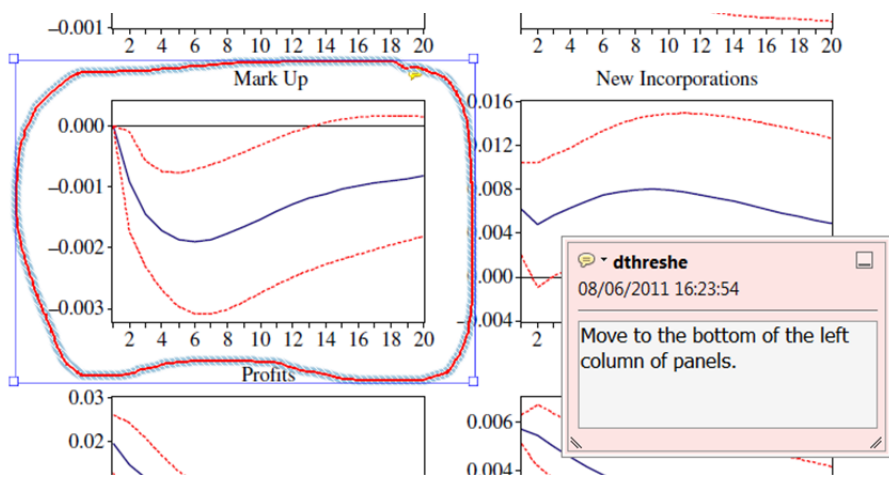


How to use it

- Click on one of the shapes in the **Drawing Markups** section.
- Click on the proof at the relevant point and draw the selected shape with the cursor.
- To add a comment to the drawn shape, move the cursor over the shape until an arrowhead appears.
- Double click on the shape and type any text in the red box that appears.

7. **Drawing Markups** Tools – for drawing shapes, lines and freeform annotations on proofs and commenting on these marks.

Allows shapes, lines and freeform annotations to be drawn on proofs and for comment to be made on these marks..



For further information on how to annotate proofs, click on the **Help** menu to reveal a list of further options:

